Electron-beam mapping of plasmon resonances in electromagnetically interacting gold nanorods

Moussa N'Gom*
Applied Physics Department and Center for Ultrafast Optical Sciences, University of Michigan—Ann Arbor, Ann Arbor, Michigan 48109, USA

Shuzhou Li and George Schatz
Department of Chemistry, Northwestern University, Evanston, Illinois 60208-3113, USA

Rolf Erni
National Center for Electron Microscopy, Lawrence Berkeley National Laboratory, 1 Cyclotron Road, MS 72-150, Berkeley, California 94720, USA

Ashish Agarwal and Nicholas Kotov
Chemical Engineering Department, University of Michigan—Ann Arbor, Ann Arbor, Michigan 48109, USA

Theodore B. Norris
EECS Department and Center for Ultrafast Optical Sciences, University of Michigan—Ann Arbor, Ann Arbor, Michigan 48109, USA
(Received 22 March 2009; revised manuscript received 11 July 2009; published 29 September 2009)

Electron energy-loss spectroscopy and energy-filtered transmission electron-microscope imaging are used to characterize the energy distribution of the surface plasmon of isolated and coupled gold nanorods. Local-field enhancement and spectral shift of the plasmon modes are observed for two interacting nanoparticles. The spatial modes measured by energy loss are shown to share qualitative similarities with the electromagnetic field distribution around gold nanorods induced by optical excitation as simulated using the discrete dipole-approximation method.

DOI: 10.1103/PhysRevB.80.113411 PACS number(s): 78.67.Bf, 07.78.+s, 02.70.Hm, 52.25.Os

Knowledge of spatial characteristics of surface-plasmon (SP) modes in noble-metal nanoparticles and nanostructures is essential for a direct control of electric field confinement in the near field. Experimental methodologies such as near-field optics and electron microscopy serve as powerful basic tools for investigation of plasmonic interactions. SP are electromagnetic excitations propagating at the interface between a dielectric and a conductor. They arise via the coupling of optical fields to oscillations of the conductor's electron plasma. Physically, these oscillations can be induced by either the driving electric field of an incident resonant optical field or impulsively by the transient field associated with a fast electron passing near a nanoparticle.

SP are used for a variety of applications such as guiding electromagnetic energy in subwavelength-sized optoelectronic devices,[1] enhanced fluorescence spectroscopy,[2] Raman spectroscopy,[3,4] near-field imaging,[5] and biosensing.[6]

Electron energy-loss spectroscopy (EELS) in a transmission electron microscope (TEM) can be used to obtain the SP spectrum by analyzing the energy of initially quasimonoenergetic electrons after they have interacted with a sample.[7] State of the art electron microscopy has achieved spatial resolution as low as 0.1 nm and energy resolution as low as ~0.2 eV.[8] For this reason, the optical plasmon modes of metallic nanoparticles have recently become accessible using EELS.

Recent experiments have shown that the dielectric function of metallic nanostructures and the mode structure required for understanding or engineering optical plasmons of a single nanoparticle can be determined via EELS.[9–11] Of course, engineered nanostructures are getting more complex, involving the coupling of simple elements to enable new functionality such as negative index materials.[12] For this reason, a number of optical spectroscopy techniques[13,14] and theoretical analyses have been used to study the distance dependence of near-field interactions between coupled systems, using both near and far-field detection. Hao *et al.*[15] theoretically considered metallic nanostructures of different shapes and sizes. Experimental studies have investigated coupled gold (Au) nanodisks in an array[16] and single-nanoparticle pairs.[17,18] To date few attempts using EELS have been made to study coupled nanoparticles and particularly their effect on the surface-plasmon modes and their ability to produce high-field enhancements.

Here, we take the next step beyond single-particle analysis[10,19] and investigate the effects of electromagnetic coupling on the SP modes of metallic nanoparticles using EELS in scanning TEM (STEM) mode. We use energy-filtered imaging (EFTEM) in order to map the SP response. We then compare the experimental plasmon intensity image obtained with this method to the calculated optical response of the same particle arrangement using the discrete dipole approximation (DDA) method.[20] The EELS data are obtained using a modified FEI Titan 80–300 microscope equipped with a special high-brightness Schottky-field emission electron source, a gun monochromator, a high-resolution GIF Tridiem energy filter, and two CEOS hexapole-type spherical aberration correctors. Whereas the STEM/EELS mapping technique has previously been used to observe the SP energy and distribution of single Au nanoparticles,[11,21] we employ EFTEM imaging to map the SP intensity of coupled Au nanorods and to show the effect of particle proximity on

the plasmon mode and to reveal field-enhancement effects that arise due to their interaction. In EFTEM mode, an adjustable energy slit is used to allow only electrons with a certain range of energies through and to form an image using these electrons on a detector.[22] EFTEM imaging has been carried out within an energy-loss range of 1–5 eV using a monochromated electron beam in combination with an energy window of 0.2 eV. The spatial sampling of the image is 512×512 pixels for a field of view of 150×150 nm. None of the data or images we present in this manuscript are processed or corrected; they are displayed as collected.

The Au nanorods are prepared using a seeding-growth method[23] with varied aspect ratio. Their optical absorption show two plasmon lines: one is due to the transverse oscillation of electrons (i.e., electron motion perpendicular to the long axis of the rods) with energy around 2.4 eV approximately coincident with the plasmon of spherical particles while the second plasmon is due to the oscillation of electrons along the long axis. This longitudinal mode is redshifted as shown in Fig. 1(c) and strongly depends on the nanostructure aspect ratio defined as the length divided by the width of the nanoparticle.[24]

A single droplet of the solution of Au nanostructures diluted in deionized water is placed on a thin SiO_x film supported on a 3-mm-diameter copper mesh TEM grid. The solvent is evaporated at room temperature. Care is taken when acquiring single-nanoparticle spectra to leave sufficient spatial separation between particles to avoid electromagnetic coupling.

The experimental EEL spectrum of a single nanorod 70-nm long and 28-nm wide is shown in Fig. 1(a). The two plasmon peaks characteristic to nanorods are displayed; the transverse peak at 2.4 eV and the longitudinal at 1.9 eV displayed in Fig. 1(d).

The loss spectrum collected at the gap of two identical Au nanorods [Fig. 1(b)] is also shown, Fig. 1(d) displays the corresponding spectrum plotted together with that of the single rod. The peak positions exhibit a significant redshift compared to the single isolated particle peak; the longitudinal peaks shift from 1.9 eV (650 nm) to 1.3 eV (950 nm) due to the coupling and the transverse peaks also experience a slight but noticeable redshift. Similar shifts to lower resonance energies have been demonstrated, when the nanoparticles are separated by a gap less than 10 nm, by a number of optical measurements on nanospheres and nanotriangles,[16–18] and theoretically by Hao and Schatz[15] for spheroidal nanoparticles. We also observe a distinct increase in the amplitude of the longitudinal peak; this is attributed to the local-field enhancement that occurs when nanostructures are close enough to strongly interact.[15,25]

We next use EFTEM to image the spatial distribution of the plasmon modes around the nanorods. Figures 2(a) and 2(b) show the longitudinal and transverse plasmon modes, respectively, of a single Au nanorod. Although methods have been developed to calculate the energy loss of an electron beam (see, for example, Refs. 26 and 27) it is interesting to investigate the relation between the spatial distribution of the energy-loss probability and the optical plasmon-mode profile. To this end, we compare our EFTEM images of the SP intensity distribution to the theoretical distribution of the

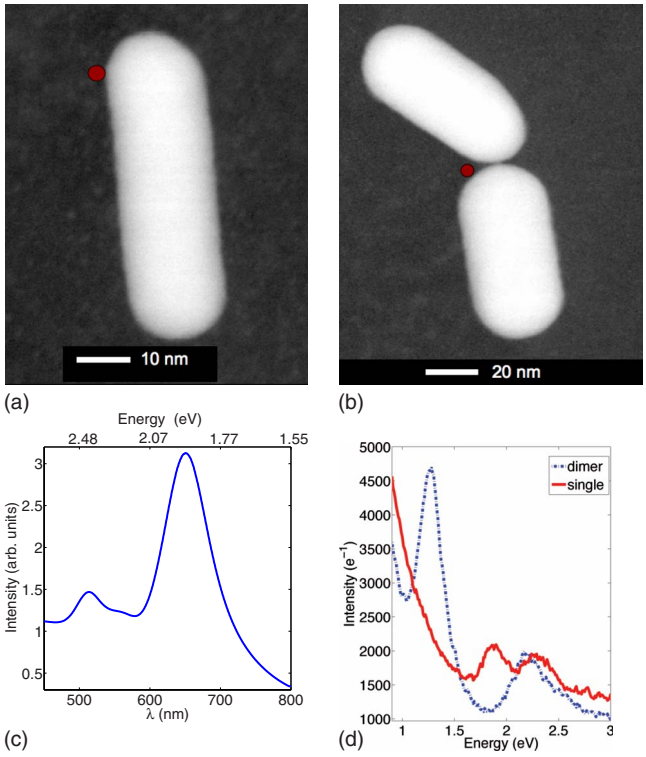

FIG. 1. (Color online) (a) Single Au nanorod with aspect ratio of 3; the red/gray dot at the edge of the particle indicate the position of the electron beam. (b) Two Au nanorods at close proximity with separation ~1 nm; here again the red/gray dot indicate the electron-beam position. (c) Ensemble optical-absorption spectrum of a solution of Au nanorods in water. The first peak at 520 nm (2.4 eV) is the main surface-plasmon absorption of Au and the second is to the longitudinal absorption of the nanorods, the observed broadening is due to the polydispersity of the sample. (d) Energy-loss spectra of a single Au nanorod, the transverse peak is at 2.4 eV, and the longitudinal peak is at 1.8 eV. The loss spectra coupled nanorods compared to the single-nanoparticle spectrum. The dipole formations show a significant redshift of the longitudinal plasmon peak and an increased electron count arising from the large-field enhancement in the dipole gap.

electromagnetic field around the particles obtained via the DDA method.[15]

All DDA calculations are performed using DDSCAT 7.0 (Ref. 28) where the grid spacing is fixed at 1 nm. The refractive index of vacuum is used and gold dielectric constants are from Johnson and Christy.[29] The Au nanoparticle is simulated by a rod with two half-sphere caps on both end, the substrate effect was considered by effective-medium approximation. The incident wavelength is 520 or 650 nm, when the electric field is parallel to either the transverse or longitudinal axis of the Au rod, respectively, to excite the corresponding plasmon mode. The square of the electric fields ($|E|^2$) around the rod are plotted. It is important to indicate that the linear value of $|E|^2$ are plotted instead of log ($|E|^2$). Figures 2(c) and 2(d) show the fields distribution around a single Au rod 70-nm long and 28-nm wide in vacuum. As can be seen by examination of the images there is good qualitative agreement between theory and experiment. Both the EFTEM images and the DDA calculations

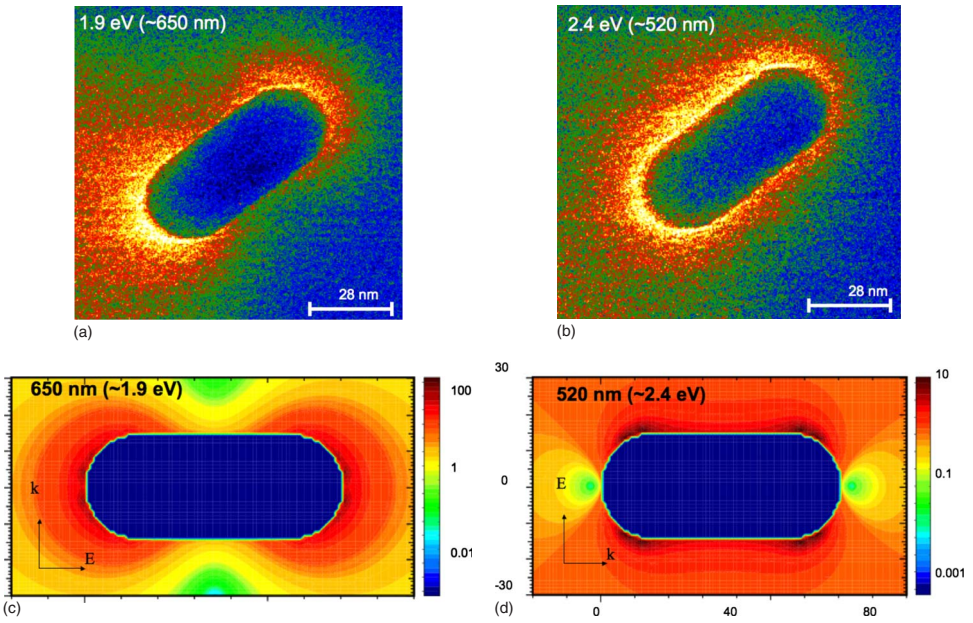

FIG. 2. (Color online) (a) EFTEM image at given energy of the spatial variation in the (a) longitudinal plasmon at 1.9 eV (corresponding to optical-transition wavelength of ~650 nm) and (b) the transverse plasmon 2.4 eV (520 nm). Theoretical distribution of the electromagnetic field around a single particle at (c) 1.9 eV (650 nm) for the longitudinal plasmon and (d) the transverse plasmon at 2.4 eV (520 nm).

reveal that the longitudinal mode shows a concentration of fields at the end of the rods whereas the transverse mode displays more uniform fields along the nanoparticle.

In Fig. 3(a) we show the EFTEM images of two nanorods with a ~5 nm gap at the given energy-loss value of 2.0 eV. The plasmon mode at the corresponding energy has its greatest concentration of fields at the edge of the nanorods with a strongly increase intensity at the gap between the particles. Similar characteristics are shown in the calculated distribution in Fig. 3(b). Both images show the same distribution of field at the edge of the particle and a higher concentration of field at the gap.

As a further test of the relation between electromagnetic mode profile and energy loss, we compare the decay of the mode amplitude away from the nanoparticle surface as determined from the EFTEM measurement and the DDA calculation. Specifically, from the data in Fig. 2(a), we extract the EFTEM intensity as a function of distance from the tip of the nanorod along the longitudinal axis over a distance up to 25 nm from the tip. Similarly, from the DDA data of Fig. 2(c), we plot the intensity $|E|^2$ along the same direction. The results are shown in Fig. 4; clearly the DDA calculation of the mode shows a similar decay of the mode intensity as the energy-loss probability.

The correspondence between the energy-loss profile and the optical-mode calculation is intriguing as it indicates the potential for EELS to access the spatial distribution of enhanced localized plasmon modes in nanostructures with spatial resolutions significantly higher than can be obtained in purely optical measurements. Recent work has begun to explore the relation between optical response and EELS; Abajo and Kociak[30] have shown that EELS loss probability is in fact given by the photonic local density of states (LDOS). The relation between $|E|^2$ and the LDOS has been considered, for example, by Girard in Ref. 31 [see Eq. (92) therein], where it is shown that scanning near-field optical microscopy (SNOM) intensities are given by the LDOS; additionally Babayan *et al.*[32] have shown that SNOM intensities in gold-ring optical corrals are accurately represented in terms of $|E|^2$ for many situations. Hence, although the rigorous relation between EELS imaging and DDA and similar calculations of optical response are yet to be firmly established, the mode profile correspondence observed in Fig. 4 is indicative of the potential of EELS for the characterization of optical plasmon modes

Indeed, Fig. 4 shows that both experimental and theoretical plots follow the same decay trend. This result is significant because this technique is able to access the spatial distribution of enhanced localized plasmon modes in nanostructure arrays with spatial resolutions orders of magnitude better than optical measurements.

The energy-loss-mode profiles are related to the optical-mode intensity because the energy lost by the incident electrons is determined by the electric fields that are induced on the nanoparticle. However for coupled particles, care should be taken when comparing field enhancements as there are important differences in the charge distribution across the particles when the plasmon is excited either impulsively by

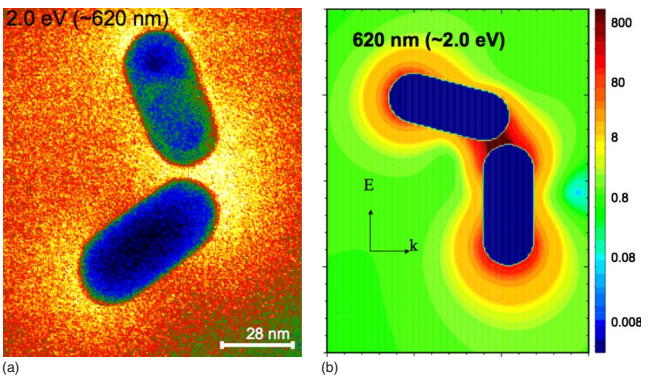

FIG. 3. (Color online) EFTEM image of spatial mode of the longitudinal (2.0 eV) plasmon of a pair of Au nanorods at close proximity with a 5-nm gap. (b) Theoretical distribution at the same energy of the longitudinal plasmon around the pair of Au nanorods.

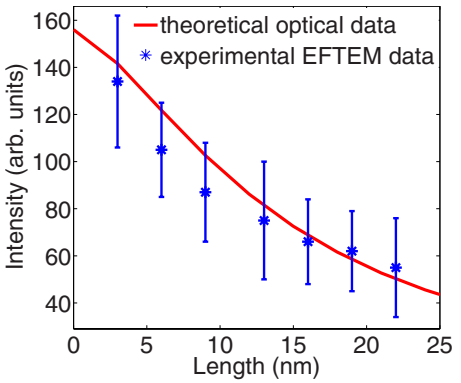

FIG. 4. (Color online) Comparison of the decay of surface-plasmon intensity obtained from the experimental EFTEM image and the optical calculations obtained using the DDA approximation. The intensity decay is measured along the longitudinal axis of the single Au nanorod.

fast moving electron for EELS or with a resonant optical pulse. Optical excitation with a polarized resonant field induces a uniform field across the two particles.[16] However, electron-beam excitation is highly localized and induces charge displacement that is related to the surface-plasmon intensity and spatial structure as the beam location is changed. For example, to characterize the plasmon mode in the gap between the nanorods, an optical excitation induces a symmetric-charge distribution across the nanoparticles; positive and negative charges alternate at the edge of the structures thus weakening the restoring forces. On the other hand when the electron beam is scanned in the gap, it induces an antisymmetric-charge distribution by repelling the negative charges from the tip of the nanorods. This formation in turn produces stronger restoring forces which in turn induces a blueshift of the plasmon peaks with respect to the optical excitation.[10] It would be interesting and valuable to extend this work to compare EELS and single-particle light scattering to quantify these effects.

In summary, we have demonstrated that EELS and EFTEM are viable methods to investigate and image the optical modes of metallic nanoparticles and coupled systems. We have shown that the spatial distribution of the plasmon modes obtained using EFTEM and optical-response simulations have similar characteristics. The advantage of using EFTEM is that it enables the detailed investigation of the field distributions of nanostructures with a resolution not accessible with conventional optical experiments.

Part of this work was performed at NCEM, which is supported by the Office of Science, Office of Basic Energy Sciences of the U.S. Department of Energy under Contract No. DE-AC0205CH11231. A.A. and N.K. would like to acknowledge the support by the AFOSR under MURI Grant No. FA9550-06-1-0337. S.L. and G.C.S. were supported by the Northwestern Materials Research Center (Grant No. DMR-0520513).

*Corresponding author. mngom@umich.edu

[1] S. A. Maier *et al.*, Appl. Phys. Lett. **81**, 1714 (2002).
[2] H. F. Hamann *et al.*, J. Chem. Phys. **114**, 8596 (2001).
[3] A. Hartschuh, E. J. Sanchez, X. S. Xie, and L. Novotny, Phys. Rev. Lett. **90**, 095503 (2003).
[4] M. Moskovits, Rev. Mod. Phys. **57**, 783 (1985).
[5] S. Takahasi and A. V. Zayats, Appl. Phys. Lett. **80**, 3479 (2002).
[6] Y. Cao *et al.*, Science **297**, 1536 (2002).
[7] R. F. Egerton, *Electron Energy Loss Spectroscopy in the Electron Microscope*, 2nd ed. (Plenum, New York, 1996).
[8] Rolf Erni and Nigel D. Browning, Ultramicroscopy **107**, 267 (2007).
[9] J. Nelayah *et al.*, Nat. Phys. **3**, 348 (2007).
[10] M. N'Gom *et al.*, Nano Lett. **8**, 3200 (2008).
[11] M. Bosman *et al.*, Nanotechnology **18**, 165505 (2007).
[12] D. R. Smith, J. B. Pendry, and M. C. K. Wiltshire, Science **305**, 788 (2004).
[13] T. Klar *et al.*, Phys. Rev. Lett. **80**, 4249 (1998).
[14] C. Sönnichsen *et al.*, Phys. Rev. Lett. **88**, 077402 (2002).
[15] E. Hao and G. C. Schatz, J. Chem. Phys. **120**, 357 (2004).
[16] W. Rechberger *et al.*, Opt. Commun. **220**, 137 (2003).
[17] K. H. Su *et al.*, Nano Lett. **3**, 1087 (2003).
[18] T. Atay *et al.*, Nano Lett. **4**, 1627 (2004).
[19] B. Schaffer, U. Hohenester, A. Trugler, and F. Hofer, Phys. Rev. B **79**, 041401(R) (2009).
[20] J. J. Goodman, B. T. Draine, and P. J. Flatau, Opt. Lett. **16**, 1198 (1991).
[21] M.-W. Chu *et al.*, Nano Lett. **9**, 399 (2009).
[22] F. Hofer, P. Warbichler, and W. Grogger, Ultramicroscopy **59**, 15 (1995).
[23] N. R. Jana and C. J. Murphy, Adv. Mater. **14**, 8082 (2002).
[24] S. Link and M. A. El-Sayed, J. Phys. Chem. B **103**, 8410 (1999).
[25] A. Sundaramurthy *et al.*, Phys. Rev. B **72**, 165409 (2005).
[26] B. L. Illman, V. E. Anderson, R. J. Warmack, and T. L. Ferrell, Phys. Rev. B **38**, 3045 (1988).
[27] F. J. García de Abajo and A. Howie, Phys. Rev. Lett. **80**, 5180 (1998).
[28] B. T. Draine and P. J. Flatau, arXiv:0809.0337 (unpublished).
[29] P. B. Johnson and R. W. Christy, Phys. Rev. B **6**, 4370 (1972).
[30] F. J. García de Abajo and M. Kociak, Phys. Rev. Lett. **100**, 106804 (2008).
[31] C. Girard, Rep. Prog. Phys. **68**, 1883 (2005).
[32] Y. Babayan *et al.*, ACS Nano **3**, 615 (2009).